

Received April 17, 2020, accepted April 30, 2020, date of publication May 7, 2020, date of current version May 21, 2020.

Digital Object Identifier 10.1109/ACCESS.2020.2992997

# Sliding Mode Control With PID Sliding Surface for Active Vibration Damping of Pneumatically Actuated Soft Robots

AMEER HAMZA KHAN<sup>1</sup> AND SHUAI LI<sup>2</sup>

<sup>1</sup>Department of Computing, The Hong Kong Polytechnic University, Hong Kong

<sup>2</sup>Department of Electronics and Electrical Engineering, College of Engineering, Swansea University, Swansea SA2 8PP, U.K.

Corresponding author: Shuai Li (shuai.li@swansea.ac.uk)

This work was supported in part by U.K. Research and Innovation (UKRI).

**ABSTRACT** This paper proposes a novel active vibration damping mechanism for soft robots. In recent years, soft robots have gained increasing research attention for robotic researchers and industrial developers alike. Soft robots offer a significant number of advantages when it comes to the handling of fragile objects, clinical rehabilitation tasks, and human-machine interaction. Soft robots demonstrate a high degree of compliance and safety because of their inherent softness, achieving the same with rigid robots will require intricate controller design and sensing mechanisms. However, the most commonly used soft robots use pneumatic systems for actuation. These pneumatic soft robots undergo large amplitude vibrations when deactivated suddenly. These vibrations not only decrease the accuracy of these soft robots but also compromise their structural integrity, which results in a decrease in their useable lifespan. An active vibration damping mechanism is very much needed to increase the utility of soft robots in industrial applications. To accurately control the dynamic behavior of soft robots, we propose a sliding mode based controller with PID sliding surface. The proposed controller uses feedback error to define a PID sliding surface, and a nonlinear sliding mode controller works to keep the system attached to the sliding surface. The coefficients of the PID sliding surface determine the dynamic behavior of the soft robot. The performance of the proposed controller is verified by using a multi-chambered parallel soft robot. The experimental results demonstrate that the proposed controller can suppress vibration amplitude to a decidedly smaller range.

**INDEX TERMS** Soft robot, sliding mode control, active damping, parallel-soft robot, multi-chambered soft robot.

## I. INTRODUCTION

Soft robots have found their applications in a wide array of areas, ranging from clinical rehabilitation robots and industrial robots to lifelike human-machine interaction systems [1]–[5]. Their softness, fast response, compliance, and low cost make them an excellent choice for safety-critical application related to the handling of delicate objects [3], [6]–[8]. Because of their inherent ability to adapt their body according to the environmental variations, they pose a low risk of damage when handling small industrial goods [9], e.g., fruits. Achieving the same level of safety and reliability with traditional rigid robots will require complex sensing mechanisms and sophisticated control techniques, which come at

very high economic cost [10]. Nevertheless, their softness and flexibility also pose a challenge when it comes to very accurate control of soft robots. Soft materials have very low damping coefficients [11], causing them to undergo large vibrations when rapidly deactivated. An example of such vibrations is illustrated in Figure 1. These vibrational transients are undesirable in industrial settings because they not only waste time in settling down, thus decreasing productivity, but also introduce structural defects in the soft robot, which reduces its useful lifespan [12], [13]. The problem of undesirable deactuation transients in soft robots require the utmost attention to increase their viability in real-world applications [14], [15].

The successful compensation of these undesirable transients requires the development of an accurate mathematical model for soft robots. Most common type of soft robots, also

The associate editor coordinating the review of this manuscript and approving it for publication was Ning Sun<sup>1</sup>.

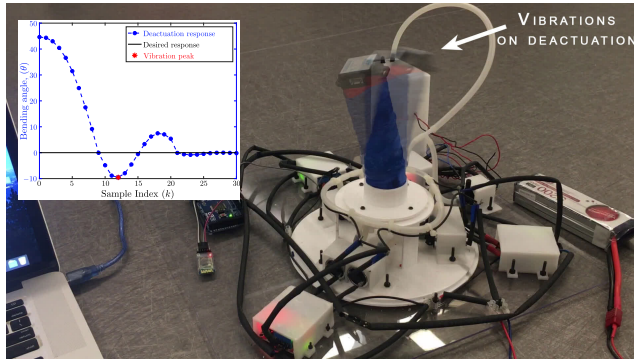


**FIGURE 1.** Figure illustrating the vibration problem in the parallel-chambered soft robot on deactuation. The soft robot move back and forth around its mean position before coming to halt.

known as pneumatic soft robots [6], [16], [17], use pneumatic system, e.g. a pump, for actuation. Pneumatic soft robots are highly nonlinear because of flexible materials and nonlinear fluid dynamics because of high-pressure airflow. Unlike rigid link robots, soft robots show an infinite degree of freedom, which theoretically requires an infinite number of parameters to formulate an exact mathematical model [18]–[20]. However, in practice, the model of the soft robot is usually approximated using a finite number of parameters using the Finite Element Method (FEM) [21]–[23]. Such a model with a large number of parameters provides a good approximation but too computationally intensive to implement on an embedded processor for real-time control. Other techniques involves using model-free control techniques e.g. a PID controller [24]. However, the PID parameter requires parameter tuning, which is a time-consuming task. Additionally, such model-free control techniques do not adapt to variations in the soft robot model and lead to an undesirable dynamic response after the inevitable degradation of the soft robot. More advanced control techniques use a low order lumped element models [18], [25]–[27] which are computationally efficient. Since such models are just a linear approximation to the actual model, these techniques required the use of error feedback to compensate for model uncertainties. Other works to induce vibration damping in pneumatic soft robots require attaching extra components to the soft robots to create mechanical damping [28], [29]. However, the extra mechanical overhead makes the system bulky and complicated to fabricate.

Linear low order model-based controller are current state of the art for soft robot control [18], [25], [30], [31]. These linear controllers are mainly focused on regulating the actuation dynamics of soft robots and do not specifically consider the deactuation dynamics and vibration problem. Consequently, these linear models struggle in suppressing the undesirable vibrations in soft robots. These nonlinear nature of soft robot models and lack of natural damping from a soft material make it challenging to suppress undesirable deactuation transients. In this paper, we propose to use a nonlinear Sliding Mode Controller (SMC) [32] to actively damp the vibrations caused

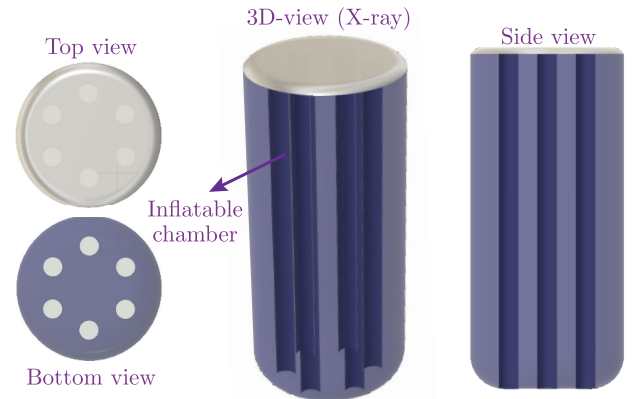


**FIGURE 2.** 3D model of the 6-chambered parallel soft robot used in our experimental platform. Left-up: Top view, left-down: bottom view, middle: transparent 3D view, right: side view.

by nonlinearities in the soft robot. The proposed sliding mode controller combined the two commonly used control techniques for soft robots; the model-free PID control and lumped element model-based control. The proposed SMC uses a PID sliding surface based on the feedback error, which combines with an approximated system model and a nonlinear control term to guarantee that the system will always remain on the sliding surface [33]. As long as the system remains on the sliding surface, the desired deactuation dynamics are produced. The nonlinear control term in the controller design is formulated such that it forces the system toward the sliding surface even in the presence of unknown model uncertainties and bounded external disturbances [34]. The convergence of the proposed controller is proved using the Lyapunov stability criterion and experimentally demonstrated using a soft robotic experimental platform [35]–[37]. [38] considered the mechanical limits of the rigid robot to constraint the state-vector in the feasible range. Such a method can also be extended to increase the reliability of soft robots.

We fabricated a 6-chambered parallel soft robot to verify the effectiveness of the proposed controller. A graphical model of the soft robot is shown in Figure 2. It contains six inflatable cylindrical chambers radially distributed inside the body of the soft robot. The robot is capable of 3-dimensional motion by controlling the input air pressure in 6 chambers. When a chamber is inflated using high-pressure air, it produces a bending motion in the soft robot in the opposite direction. By controlling the air pressure inside these chambers, the bending angle and orientation of the soft robot can be controlled. We constructed a complete soft robotic platform consisting of pumps, valves, MOSFET switches, and micro-controllers. The detail of the experimental platform is given in the subsequent sections. The experimental platform is shown in Figure 1. The highlights and contribution of this paper are summarized below

- 1) Active vibration damping of the soft robots by formulating an SMC controller with PID based sliding surface. The nonlinear switching term introduced by the

SMC controller assist in compensating for unmodelled nonlinearities.

- 2) The convergence and stability of the controller are proved rigorously using theoretical analysis based on the Lyapunov function.
- 3) The design of a novel 6-chambered parallel soft robots is presented. The robot is used as an experimental platform to demonstrate the efficacy of the proposed controller.

The remaining paper is organized as follow: Section II describe the physical and mathematical model of the soft robot, Section III provides the formulation of sliding mode controller and proof of its convergence, Section IV present experimental results and Section V concludes the paper.

## II. SOFT ROBOT MODEL

In this section, we will discuss the structure of our soft robot, construction of the experimental platform, and formulation of a mathematical model that will be used in developing the SMC based controller.

### A. PARALLEL SOFT ROBOT

To fabricate the soft parallel robot, we designed the molds according to the structure of our soft robot and used a 3D printer to create those molds. We used Ecoflex-30 silicone [39] as the material for our soft robot because of its high flexibility and low cost. The liquid silicone mixture was prepared and poured in the molds and left for curing in the open air for about 8 hours to let the mixture dry completely. We removed the soft robot from the molds and inserted silicone tubes into the chambers to inflate them using an external pressure source. We then mounted the soft robot on the experimental platform, as shown in Figure 3(a).

We used a 12V DC vacuum pump to power the soft robot. In order to control the bending angle of the soft robot, the air pressure from the pump to the soft robot needs to be regulated. Therefore, we attached solenoid valves between the pump and chambers of the soft robots. The solenoid valves are 3-position 3-port, i.e., they can exist in 3 states; inflating, holding the air, and deflating the soft robot chambers. By controlling the state of the valve, the air pressure inside each of the valves can be regulated.

For the digital implementation of the control algorithm, we used an ATmega-2560. The controller pins generate signals for controlling the state of the solenoid valves. Since the pins of ATmega-2560 can provide few milliamperes (mA) of currents, which is insufficient to drive the solenoid valves directly, we used MOSFET switches to provide adequate currents. MOSFET switches can provide very high output switching current and consume small input current from the microcontroller. The gate input of the MOSFET switches was connected to the microcontroller pins. To program the ATmega-2560, we implemented the controller on Simulink [40], [41] and then used the Simulink Support Package for Arduino target to directly program the microcontroller. This approach increases the efficiency of system development

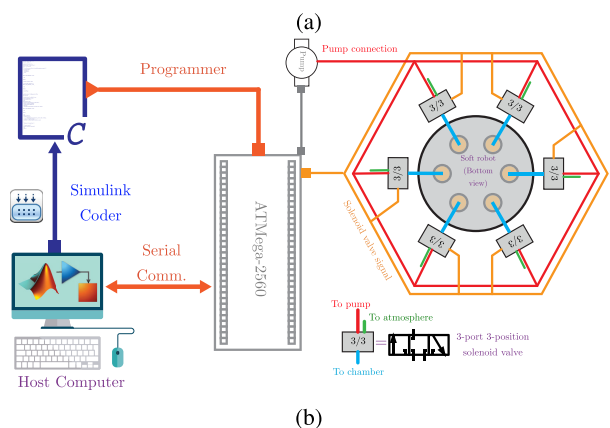
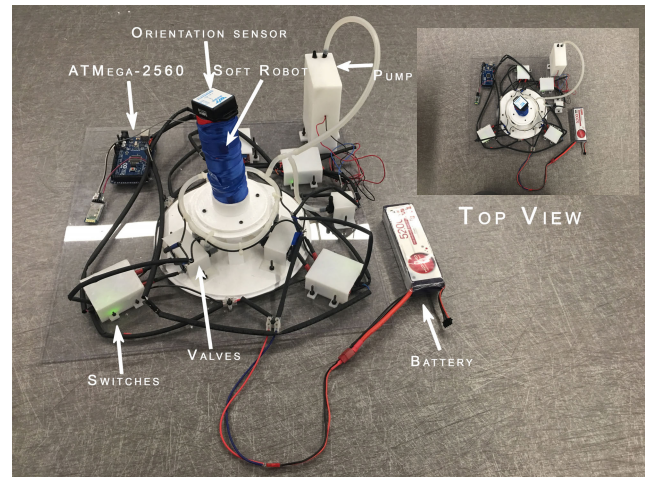


**FIGURE 3.** Experimental platform for our soft robot. (a) Labeled image of the experimental platform. (b) Schematic diagram of the soft robot, showing relationship between different components of the experimental platform.

since it automatically generates a reliable code and help in avoiding the tedious task of manually writing and debugging the controller code.

To sense the bending motion of the soft robot, we mounted a wireless orientation sensor to the top of the soft robot, as shown in Figure 3(a). The sensor directly measures the magnitude of the bending angle relative to the vertical position of the soft robot. When the soft robot is deactuated, i.e., vertical position, the orientation sensor gives zero value. Otherwise, its value is proportional to the bending angle. The orientation sensor is connected to the ATmega-2560 controller using a Bluetooth module. The schematic diagram of the experimental platform and the connection between parts is shown in Figure 3(b).

### B. DYNAMIC MODELLING

Our soft robot has six identical chambers, and for the sake of simplicity, we will only consider a single chamber in the dynamic modeling. Additionally, since we are mainly concerned about suppressing the deactuation transients, analyzing the dynamic behavior of a single chamber will provide



enough information while keeping the discussion simple. The dynamic model of a single chamber of the soft robot using lumped element method can be described as a second-order dynamic system as follow:

$$a_1\ddot{\theta}(t) + a_2\dot{\theta}(t) + a_3\theta(t) = u(t), \quad (1)$$

where  $\theta(t)$  is the magnitude of bending angle,  $a_1, a_2, a_3$  are the constant model parameters and  $u(t)$  is the input pressure to chamber.

Equation (1) represents a second-order dynamic model, which is a linear approximation to the actual model of the soft robot. To account for unmodelled nonlinearities, we treat them as perturbations to the linear model (1). Similarly, unknown external disturbances can also induce instability in the soft robot. We add the combined effect of perturbation and unknown external disturbances to the system model as follow:

$$a_1\ddot{\theta}(t) + a_2\dot{\theta}(t) + a_3\theta(t) = u(t) + d(t), \quad (2)$$

where  $d(t)$  represent the combination of perturbations, model Uncertainties and unknown external disturbances.

To estimate the system parameters  $a_1, a_2, a_3$  we used MATLAB's system identification toolbox [42]. The toolbox requires the application of a periodic input signal and use the measured output values to estimate the system parameters. We ran a periodic inflate-hold-deflate experiment, over the entire range of operating pressure, for a chamber of the soft robot, the measured values are shown in Figure 4. These estimated values for the parameters are  $a_1 = 8.2 \times 10^{-5}$ ,  $a_2 = 1.1 \times 10^{-3}$ ,  $a_3 = 2.4 \times 10^{-2}$ .

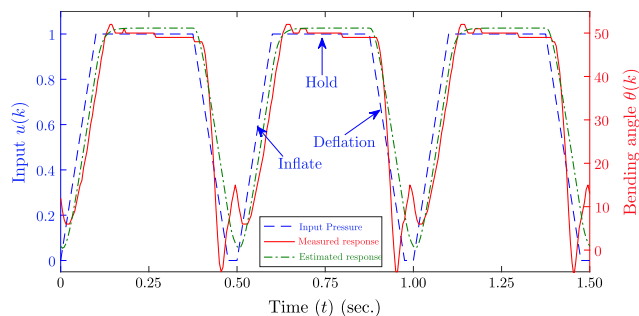


**FIGURE 4.** System response for the experiment conducted to estimate the system model parameters  $a_1, a_2, a_3$ . The experiment consisted of inflate-hold-release cycle for a chamber of the soft robot. The output of the estimated model (green) is very close to the measured output (red), depicting the accuracy of the estimated model. (Sampling interval:  $T_s = 0.005$ ).

### III. SMC CONTROLLER DESIGN

In this section, we will present the scheme of our proposed SMC controller for the soft robotic platform.

#### A. CONTROLLER FORMULATION

The system model defined by (2) contains an unknown term  $d(t)$  which accounts for unmodelled perturbations and external disturbances. We used one-step delayed calculation to

estimate perturbations  $d(t)$  in real-time as follow:

$$\begin{aligned} \hat{d}(t) &= d(t_{-1}) \\ &= a_1\ddot{\theta}(t_{-1}) + a_2\dot{\theta}(t_{-1}) + a_3\theta(t_{-1}) - u(t_{-1}) \end{aligned} \quad (3)$$

where  $t_{-1} = t - T_s$  is used to denote the previous time-step,  $T_s$  is the sampling period for the controller.  $\hat{d}(t)$  denotes the estimation for perturbation at time instant  $t$ . The first order and second-order derivative terms are calculates using first and second-order backward difference methods, i.e.,

$$\begin{aligned} \dot{\theta}(t_{-1}) &\approx \frac{\theta(t_{-1}) - \theta(t_{-2})}{T_s} \\ \ddot{\theta}(t_{-1}) &\approx \frac{\theta(t_{-1}) - 2\theta(t_{-2}) + \theta(t_{-3})}{T_s} \end{aligned}$$

The equation (3) uses past observation to generate an estimate for perturbation in the current time step. In practice the  $T_s$  is small enough that  $d(t) \approx d(t - T_s)$ , therefore  $\hat{d}(t)$  gives a reliable approximation for  $d(t)$ . By using the above estimation, we can write the system model as follow,

$$a_1\ddot{\theta}(t) + a_2\dot{\theta}(t) + a_3\theta(t) = u(t) + \hat{d}(t) + \tilde{d}(t) \quad (4)$$

where  $\tilde{d}(t) = d(t) - \hat{d}(t)$  represents the error between the real and estimated perturbation at time instant  $t$ .

To design the SMC controller, we defined the error coordinates as follows,

$$e(t) = \theta(t) - \theta_d(t) \quad (5)$$

where  $\theta(t)$  is the current bending angle and  $\theta_d(t)$  is the desired bending angle.

Based on the defined error coordinates, we defined a PID-type sliding mode function as follow:

$$s(t) = \dot{e}(t) + k_1e(t) + k_2 \int_0^t e(\tau) d\tau \quad (6)$$

where  $k_1$  and  $k_2$  are the design parameters to tune the dynamic response of the system on the sliding surface. While choosing these parameters, it should be noted that the characteristics polynomial  $s^2 + k_1s + k_2 = 0$  should be strictly Hurwitz. The sliding mode controller is designed such that it keeps the system close to the sliding surface  $s(t) = 0$ . As long as the system remains on the sliding surface, the desired dynamic response is obtained. Note that for the sake of brevity, the time dependence variable ( $t$ ) will be omitted in the following discussion.

*Theorem:* For the system (4) with the sliding surface defined by (6), the angle tracking error  $e$  will asymptotically converge to 0 i.e.  $\lim_{t \rightarrow \infty} e = 0$  if control input  $u$  is governed by following equation:

$$\begin{aligned} u &= (a_2 - k_1a_1)\dot{\theta} + (a_3 - k_2a_1)\theta - \hat{d} \\ &\quad + a_1(\ddot{\theta}_d + k_1\dot{\theta}_d + k_2\theta_d) - \eta \text{sign}(s) \end{aligned} \quad (7)$$

where  $\text{sign}(\cdot)$  is the signum function,  $\eta$  is switching gain, and  $\eta \text{sign}(s)$  is the nonlinear control term to always force the system toward the sliding surface even when uncertainties drive it away.

*Proof:* Defining  $V = a_1 s^2/2$  as a positive definite Lyapunov function, whose first derivative is given by

$$\dot{V} = a_1 s \dot{s}. \quad (8)$$

To obtain  $\dot{s}$ , we take the derivative of  $s$  as defined in (6), and use (4) to replace  $\ddot{\theta}$ , which results in

$$\begin{aligned} \dot{s} &= \ddot{e} + k_1 \dot{e} + k_2 e \\ &= \left(k_1 - \frac{a_2}{a_1}\right) \dot{\theta} + \left(k_2 - \frac{a_3}{a_1}\right) \theta + \frac{1}{a_1} u \\ &\quad + \frac{1}{a_1} (\hat{d} + \tilde{d}) - \ddot{\theta}_d - k_1 \dot{\theta}_d - k_2 \theta_d. \end{aligned}$$

Replacing the expression for  $\dot{s}$  in (8) we get the following expression,

$$\begin{aligned} \dot{V} &= a_1 \left(k_1 - \frac{a_2}{a_1}\right) \dot{\theta} s + a_1 \left(k_2 - \frac{a_3}{a_1}\right) \theta s + us \\ &\quad + (\hat{d} + \tilde{d}) s - a_1 (\ddot{\theta}_d + k_1 \dot{\theta}_d + k_2 \theta_d) s. \end{aligned}$$

Now replacing the value of control input  $u$  in above expression and simplifying, we get,

$$\begin{aligned} \dot{V} &= -\eta \text{sign}(s) s + \tilde{d} s \\ &= -\eta |s| + \tilde{d} s. \end{aligned} \quad (9)$$

From (9) it can be deduced that if we choose  $\eta$  such that

$$\eta > |\tilde{d}| + \epsilon, \quad (10)$$

then  $\dot{V} < -\epsilon |s|$  for all values of  $s$ . Here  $\epsilon$  is an arbitrary positive constant. Since  $\dot{V}$  is negative, which proves that the tracking error  $e$  will eventually converge to 0, i.e., the system states  $\theta$  will reach the sliding surface  $s = 0$ . Besides, this also proves that once the system reaches the sliding surface, it will remain to confide to it because leaving the sliding surface will violate the in inequality (10). Therefore, the choice of  $\eta$  should be such that it is greater than the bound on uncertainties error of  $\tilde{d}$ . Remember that  $\tilde{d}$  is just the perturbation estimation error, which is usually much smaller than the perturbation  $d$  itself. Therefore the proposed controller is much better in regulating the dynamic response of the soft robot. The upper bound on the perturbation estimation error can be found by exciting the system with a known input signal and recording the output value. Then, observed values can be used to estimate the model parameters  $a_1$ ,  $a_2$ , and  $a_3$  in (1). The difference in the estimated model and the observed data can be used to estimate the empirical upper bound on the disturbance.

*Remark:* Because the  $\text{sign}(\cdot)$  function is discontinuous, it may introduce a lot of chattering in the control signal  $u$ . To avoid this issue, by following the approach of [43] it is often desirable to use the saturation function  $\text{sat}(\cdot)$  as a soft alternate to  $\text{sign}(\cdot)$ .  $\text{sat}(\cdot)$  is defined as,

$$\text{sat}(s) = \begin{cases} \text{sign}(s), & \text{for } |s| > \delta \\ s/\delta & \text{for } |s| \leq \delta, \end{cases}$$

where  $\delta$  is a design parameter, as  $\delta$  approaches 0, the  $\text{sat}(\cdot)$  become similar to  $\text{sign}(\cdot)$  function. The  $\text{sat}(\cdot)$  will keep the

soft robot states in the vicinity of the sliding surface. The choice of the value of  $\delta$  is a compromise between the chattering and magnitude of tracking error.

## IV. EXPERIMENTS & RESULTS

In this section, we will explain the experimental methodology and discuss the results. The soft robot response demonstrates that the proposed controller is effective in regulating the dynamic response and actively suppressing the vibrations on deactuation.

### A. SIMULATION RESPONSE

We carried out an extensive set of simulations to study the effect of different controller parameters on the dynamic response of the soft robots. We used Simulink for carrying out numerical simulations. We implemented the system model and SMC based controller in Simulink, which, in addition to simulations, was directly used to program our microcontroller by using automatic code generation. We carried out three different sets of simulations to study the effect of control parameters  $k_1$ ,  $k_2$ , and  $\eta$  on dynamic response during deactuation. The simulation responses are shown in Figure 5.

Figure 5(a) shows the results of simulations on using different values of  $k_1$  while other parameters remain constant. These results show that the dynamic response becomes damped, and vibration amplitude decrease as the value of  $k_1$  increases. However, large values tend to show a slower response. Similarly, Figure 5(b) shows the results of simulations on using different values of  $k_2$ . These results show that the dynamic response becomes damper as the value of  $k_2$  becomes small. In this case, a small value of  $k_2$  tends to show a very sluggish response.

The effect of switching gain  $\eta$  on the dynamic system response is shown in Figure 5(c). The response shows that the dynamic response becomes more damped as the value of  $k_1$  decreases. However, using smaller values tends to have a small impact on the dynamic response. This can be explained based on the fact that  $\eta$  is a nonlinear switching gain, which only ensures the asymptomatic convergence, but does not directly impact the dynamic response. However, a large value of  $\eta$  can leads to aggressive system behavior because of its large contribution to the control signal  $u(t)$ , as shown in Figure 5(c).

### B. EXPERIMENTAL RESULTS

Now we will present the experimental results conducted on our soft robotic platform shown in Figure 3(a). We set the sampling interval  $T_s$  to 0.005 seconds. Small value of sampling interval ensure the assumption made in perturbation estimation i.e.  $\hat{d}(t) = d(t - T_s) \approx d(t)$ , remains true. The experimental results are summarized in Figure 6.

We first experimented using a PID controller to obtain a baseline for measuring the performance of the proposed controller. The experiment involved releasing the soft robot from an initial bending position of  $\theta = 45^\circ$  and measuring the vibration amplitude on reaching the deactuation position

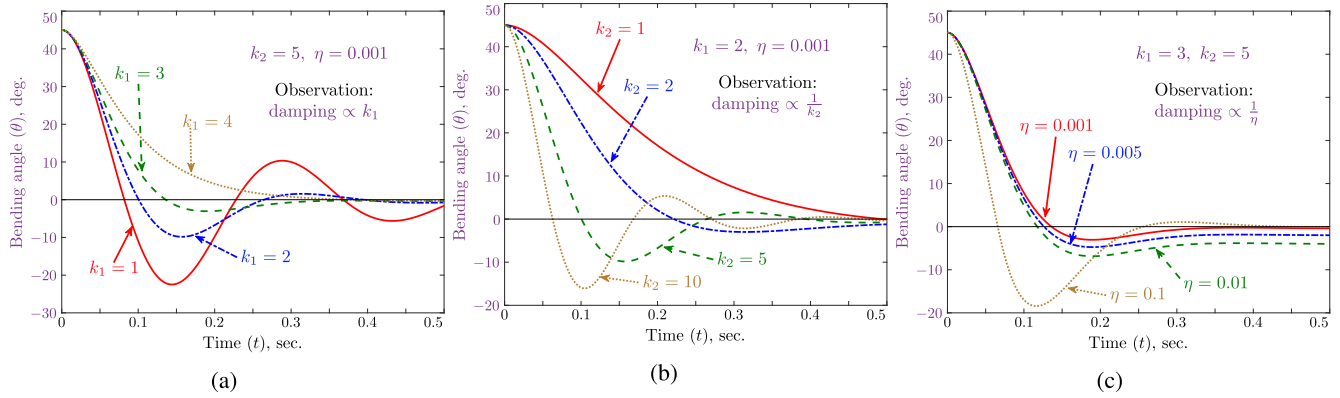


**FIGURE 5.** Simulated response for different values of parameters  $k_1, k_2$ , and  $\eta$ . (a) As  $k_1$  increase the vibration damping also increase. (b) Dynamic response is more damped for small values of  $k_2$ . (c) If  $\eta$  becomes too large than the vibration amplitude increases. However, asymptomatic convergence is shown in all the cases.

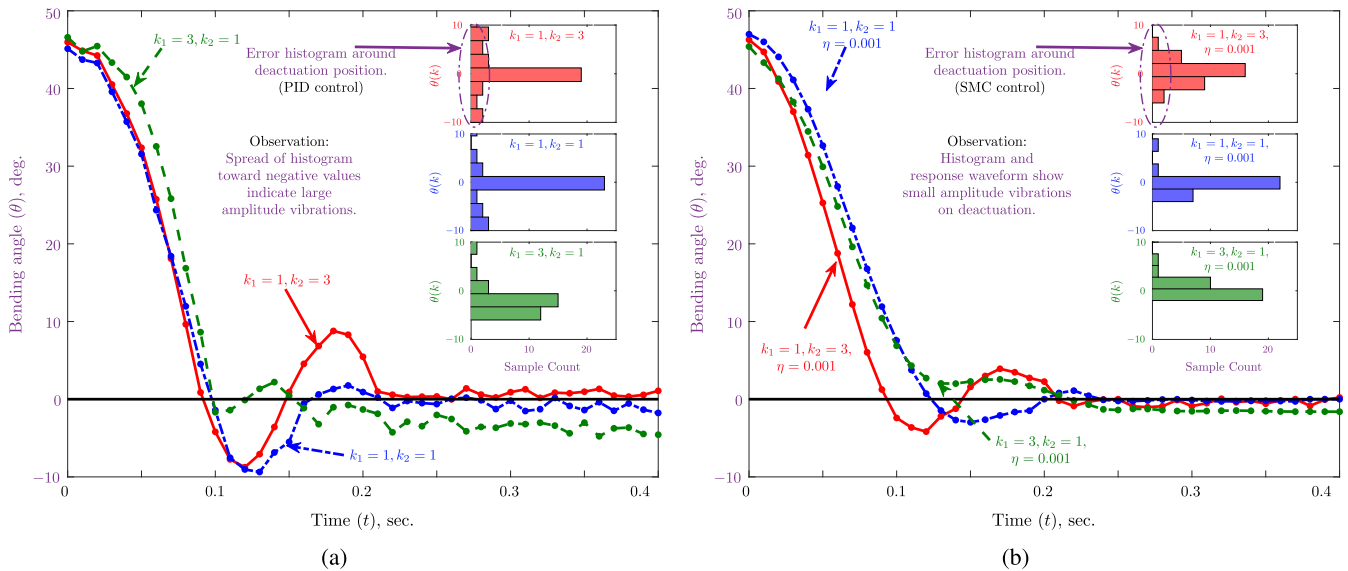


**FIGURE 6.** Experimental results and comparison between the performance of a PID controller and the proposed SMC based controller. (a) The performance of the PID controller for three different values of parameters, the response shows large vibrations on deactuation. (b) The response of the proposed SMC controller with PID sliding surface. It can be seen that the proposed controller create small vibrations as compared to PID, for same parameter values.

( $\theta = 0^\circ$ ). The experiments were conducted using different values of PID parameters. Three of the responses are shown in Figure 6(a). It can be seen from the waveforms that the soft robot overshoot up to a maximum angle of  $-8^\circ$  before coming to a halt. Figure 6(b) also shows error histogram for three trials with  $\theta_d = 0$ . It can be seen that the histograms are largely spread out toward negative values, which indicate the presence of overshoot and vibrations.

We then conducted the experiments using our proposed SMC based controller using the PID sliding surface. Again the initial angle was set to  $45^\circ$ . The experiments were repeated using different values of parameters. The response is shown in Figure 6(b) have similar parameter values as the PID responses, with addition of nonlinear switching gain parameter  $\eta = 0.001$ . It can be seen that the proposed controller can dampen out the vibrations as compared to the PID controller.

For a similar value of  $k_1$  and  $k_2$ , the response shown by the proposed controller is much smaller as compared to the PID controller. The error histograms are shown in Figure 6(b) also shows that the error is concentrated near  $\theta = 0$ , and large negative values have very rear occurrence.

## V. CONCLUSION

In this paper, we proposed a practical solution for dynamic response regulation and vibration damping problem for soft robots. We formulated a nonlinear sliding mode controller based on a PID type sliding surface. The presented controller combines the advantages of two primary control approaches presented in soft robotic literature, i.e., model-free PID controller and lumped element model-based controllers. The nonlinear term in the proposed controller plays an essential role in confining the states of the soft robot on the sliding

surface, even in the presence of model uncertainties and unknown external disturbance. The controller uses an effective perturbation estimation technique, which makes it easy to tune the controller parameters. We theoretically proved the convergence of the proposed controller using the Lyapunov stability criterion. We demonstrated its performance using extensive simulation and experimental results on our six-chambered soft parallel robot. To the best of our knowledge, this is the first work to apply a sliding mode controller for active vibration damping of soft robots.

## REFERENCES

- [1] M. Cianchetti, C. Laschi, A. Menciassi, and P. Dario, "Biomedical applications of soft robotics," *Nature Rev. Mater.*, vol. 3, no. 6, pp. 143–153, Jun. 2018.
- [2] M. Manti, T. Hassan, G. Passetti, N. D'Elia, C. Laschi, and M. Cianchetti, "A bioinspired soft robotic gripper for adaptable and effective grasping," *Soft Robot.*, vol. 2, no. 3, pp. 107–116, Sep. 2015.
- [3] H. Lin, F. Guo, F. Wang, and Y.-B. Jia, "Picking up a soft 3D object by 'feeling' the grip," *Int. J. Robot. Res.*, vol. 34, no. 11, pp. 1361–1384, 2015.
- [4] P. Polygerinos, S. Lyne, Z. Wang, L. F. Nicolini, B. Mosadegh, G. M. Whitesides, and C. J. Walsh, "Towards a soft pneumatic glove for hand rehabilitation," in *Proc. IEEE/RSJ Int. Conf. Intell. Robots Syst. (IROS)*, Nov. 2013, pp. 1512–1517.
- [5] I. Galiana, F. L. Hammond, R. D. Howe, and M. B. Popovic, "Wearable soft robotic device for post-stroke shoulder rehabilitation: Identifying misalignments," in *Proc. IEEE/RSJ Int. Conf. Intell. Robots Syst. (IROS)*, Oct. 2012, pp. 317–322.
- [6] Y. Hao, Z. Gong, Z. Xie, S. Guan, X. Yang, Z. Ren, T. Wang, and L. Wen, "Universal soft pneumatic robotic gripper with variable effective length," in *Proc. 35th Chin. Control Conf. (CCC)*, Jul. 2016, pp. 6109–6114.
- [7] C. Yang, G. Peng, Y. Li, R. Cui, L. Cheng, and Z. Li, "Neural networks enhanced adaptive admittance control of optimized robot–environment interaction," *IEEE Trans. Cybern.*, vol. 49, no. 7, pp. 2568–2579, Jul. 2019.
- [8] H. Wang, P. X. Liu, X. Xie, X. Liu, T. Hayat, and F. E. Alsaadi, "Adaptive fuzzy asymptotical tracking control of nonlinear systems with unmodeled dynamics and quantized actuator," *Inf. Sci.*, early access, Apr. 3, 2018, doi: 10.1016/j.ins.2018.04.011.
- [9] C. Yang, J. Luo, C. Liu, M. Li, and S.-L. Dai, "Haptics electromyography perception and learning enhanced intelligence for teleoperated robot," *IEEE Trans. Autom. Sci. Eng.*, vol. 16, no. 4, pp. 1512–1521, Oct. 2019.
- [10] L. R. Hochberg, D. Bacher, B. Jarosiewicz, N. Y. Masse, J. D. Simeral, J. Vogel, S. Haddadin, J. Liu, S. S. Cash, P. van der Smagt, and J. P. Donoghue, "Reach and grasp by people with tetraplegia using a neurally controlled robotic arm," *Nature*, vol. 485, no. 7398, pp. 372–375, May 2012.
- [11] C. W. De Silva, *Vibration Damping, Control, and Design*. Boca Raton, FL, USA: CRC Press, 2007.
- [12] S. Terry, J. Brancart, D. Lefeber, G. Van Assche, and B. Vanderborght, "Self-healing soft pneumatic robots," *Sci. Robot.*, vol. 2, no. 9, p. eaan4268, Aug. 2017.
- [13] H. Wang, P. X. Liu, X. Zhao, and X. Liu, "Adaptive fuzzy finite-time control of nonlinear systems with actuator faults," *IEEE Trans. Cybern.*, vol. 50, no. 5, pp. 1786–1797, May 2020.
- [14] S. Ling, H. Wang, and P. X. Liu, "Adaptive fuzzy dynamic surface control of flexible-joint robot systems with input saturation," *IEEE/CAA J. Automatica Sinica*, vol. 6, no. 1, pp. 97–107, Jan. 2019.
- [15] L. Cheng, W. Liu, C. Yang, T. Huang, Z.-G. Hou, and M. Tan, "A neural-network-based controller for piezoelectric-actuated stick–slip devices," *IEEE Trans. Ind. Electron.*, vol. 65, no. 3, pp. 2598–2607, Mar. 2018.
- [16] M. Doumit, A. Fahim, and M. Munro, "Analytical modeling and experimental validation of the braided pneumatic muscle," *IEEE Trans. Robot.*, vol. 25, no. 6, pp. 1282–1291, Dec. 2009.
- [17] N. Sun, D. Liang, Y. Wu, Y. Chen, Y. Qin, and Y. Fang, "Adaptive control for pneumatic artificial muscle systems with parametric uncertainties and unidirectional input constraints," *IEEE Trans. Ind. Informat.*, vol. 16, no. 2, pp. 969–979, Feb. 2020.
- [18] C. D. Santina, R. K. Katzschmann, A. Biechi, and D. Rus, "Dynamic control of soft robots interacting with the environment," in *Proc. IEEE Int. Conf. Soft Robot. (RoboSoft)*, Apr. 2018, pp. 46–53.
- [19] Y. Zhang, Z. Qi, B. Qiu, M. Yang, and M. Xiao, "Zeroing neural dynamics and models for various time-varying problems solving with ZLSF models as minimization-type and euler-type special cases [research frontier]," *IEEE Comput. Intell. Mag.*, vol. 14, no. 3, pp. 52–60, Aug. 2019.
- [20] Y. Shi and Y. Zhang, "Solving future equation systems using integral-type error function and using twice ZNN formula with disturbances suppressed," *J. Franklin Inst.*, vol. 356, no. 4, pp. 2130–2152, Mar. 2019.
- [21] A. D. Marchese, C. D. Onal, and D. Rus, "Autonomous soft robotic fish capable of escape maneuvers using fluidic elastomer actuators," *Soft Robot.*, vol. 1, no. 1, pp. 75–87, Mar. 2014.
- [22] F. Largilliere, V. Verona, E. Coevoet, M. Sanz-Lopez, J. Dequidt, and C. Duriez, "Real-time control of soft-robots using asynchronous finite element modeling," in *Proc. IEEE Int. Conf. Robot. Automat. (ICRA)*, May 2015, pp. 2550–2555.
- [23] J. Na, M. N. Mahyuddin, G. Herrmann, X. Ren, and P. Barber, "Robust adaptive finite-time parameter estimation and control for robotic systems," *Int. J. Robust Nonlinear Control*, vol. 25, no. 16, pp. 3045–3071, Nov. 2015.
- [24] G. Gerboni, A. Diodato, G. Ciuti, M. Cianchetti, and A. Menciassi, "Feedback control of soft robot actuators via commercial flex bend sensors," *IEEE/ASME Trans. Mechatronics*, vol. 22, no. 4, pp. 1881–1888, Aug. 2017.
- [25] E. H. Skorina, M. Luo, W. Tao, F. Chen, J. Fu, and C. D. Onal, "Adapting to flexibility: Model reference adaptive control of soft bending actuators," *IEEE Robot. Autom. Lett.*, vol. 2, no. 2, pp. 964–970, Apr. 2017.
- [26] H. Wang, B. Yang, Y. Liu, W. Chen, X. Liang, and R. Pfeifer, "Visual servoing of soft robot manipulator in constrained environments with an adaptive controller," *IEEE/ASME Trans. Mechatronics*, vol. 22, no. 1, pp. 41–50, Feb. 2017.
- [27] W. He, H. Huang, and S. S. Ge, "Adaptive neural network control of a robotic manipulator with time-varying output constraints," *IEEE Trans. Cybern.*, vol. 47, no. 10, pp. 3136–3147, Oct. 2017.
- [28] Y. Wei, Y. Chen, T. Ren, Q. Chen, C. Yan, Y. Yang, and Y. Li, "A novel, variable stiffness robotic gripper based on integrated soft actuating and particle jamming," *Soft Robot.*, vol. 3, no. 3, pp. 134–143, Sep. 2016.
- [29] Y. Li, Y. Chen, T. Ren, and Y. Hu, "Passive and active particle damping in soft robotic actuators this work is funded by a basic research grant from the University of Hong Kong," in *Proc. IEEE Int. Conf. Robot. Automat. (ICRA)*, May 2018, pp. 1547–1552.
- [30] T. G. Thuruthel, E. Falotico, F. Renda, and C. Laschi, "Model-based reinforcement learning for closed-loop dynamic control of soft robotic manipulators," *IEEE Trans. Robot.*, vol. 35, no. 1, pp. 124–134, Feb. 2019.
- [31] W. Felt, K. Y. Chin, and C. D. Remy, "Contraction sensing with smart braid McKibben muscles," *IEEE/ASME Trans. Mechatronics*, vol. 21, no. 3, pp. 1201–1209, Jun. 2016.
- [32] X. Yu, B. Wang, and X. Li, "Computer-controlled variable structure systems: The state-of-the-art," *IEEE Trans. Ind. Informat.*, vol. 8, no. 2, pp. 197–205, May 2012.
- [33] J. Na, X. Ren, and D. Zheng, "Adaptive control for nonlinear pure-feedback systems with high-order sliding mode observer," *IEEE Trans. Neural Netw. Learn. Syst.*, vol. 24, no. 3, pp. 370–382, Mar. 2013.
- [34] J. Na, B. Jing, Y. Huang, G. Gao, and C. Zhang, "Unknown system dynamics estimator for motion control of nonlinear robotic systems," *IEEE Trans. Ind. Electron.*, vol. 67, no. 5, pp. 3850–3859, May 2020.
- [35] Y. Zhang, Z. Qi, M. Yang, J. Guo, and H. Huang, "Step-width theoretics and numerics of four-point general DTZN model for future minimization using jury stability criterion," *Neurocomputing*, vol. 357, pp. 231–239, Sep. 2019.
- [36] W. He, Z. Yin, and C. Sun, "Adaptive neural network control of a marine vessel with constraints using the asymmetric barrier Lyapunov function," *IEEE Trans. Cybern.*, vol. 47, no. 7, pp. 1641–1651, Jul. 2017.
- [37] C. Yang, Y. Jiang, Z. Li, W. He, and C.-Y. Su, "Neural control of bimanual robots with guaranteed global stability and motion precision," *IEEE Trans. Ind. Informat.*, vol. 13, no. 3, pp. 1162–1171, Jun. 2017.
- [38] H. Chen and N. Sun, "Nonlinear control of underactuated systems subject to both actuated and unactuated state constraints with experimental verification," *IEEE Trans. Ind. Electron.*, early access, Oct. 15, 2019, doi: 10.1109/TIE.2019.2946541.
- [39] Smooth-On Inc. *Dragon Skin 20*. Accessed: Aug. 28, 2018. [Online]. Available: <https://www.smooth-on.com/products/dragon-skin-20/>



- [40] D. Xue and Y. Chen, *Modeling, Analysis and Design of Control Systems in MATLAB and Simulink*. Singapore: World Scientific, 2015.
- [41] Y. Li and Q. Xu, "Adaptive sliding mode control with perturbation estimation and PID sliding surface for motion tracking of a piezo-driven micromanipulator," *IEEE Trans. Control Syst. Technol.*, vol. 18, no. 4, pp. 798–810, Jul. 2010.
- [42] L. Ljung, "MATLAB: System identification toolbox: User's guide version 4," Mathworks, Natick, MA, USA, Tech. Rep., 1995.
- [43] Q. Xu, "Adaptive discrete-time sliding mode impedance control of a piezo-electric microgripper," *IEEE Trans. Robot.*, vol. 29, no. 3, pp. 663–673, Jun. 2013.



**AMEER HAMZA KHAN** received the B.S. degree in electrical engineering from the Pakistan Institute of Engineering and Applied Sciences, Islamabad, Pakistan, in 2015. He is currently pursuing the Ph.D. degree in optimal control of robotic systems with the Department of Computing, The Hong Kong Polytechnic University, Hong Kong.

He was a Research Assistant with the Department of Computing, The Hong Kong Polytechnic University. His research interests include nonlinear

optimization, metaheuristic algorithms, adaptive control, and machine learning.



**SHUAI LI** received the B.E. degree in precision mechanical engineering from the Hefei University of Technology, Hefei, China, in 2005, the M.E. degree in automatic control engineering from the University of Science and Technology of China, Hefei, in 2008, and the Ph.D. degree in electrical and computer engineering from the Stevens Institute of Technology, Hoboken, NJ, USA, in 2014. He is currently leading the Robotic Lab, conducting research on robot manipulation and impedance control, multirobot coordination, distributed control, intelligent optimization and control, and legged robots. He is the founding Editor-in-Chief of the *International Journal of Robotics and Control* and the General Co-Chair of the 2018 International Conference on Advanced Robotics and Intelligent Control.

• • •